Veterinary Microbiology 239 (2019) 108456

Contents lists available at ScienceDirect

Veterinary Microbiology

journal homepage: www.elsevier.com/locate/vetmic

Cholesterol 25-Hydroxylase inhibits bovine parainfluenza virus type 3 replication through enzyme activity-dependent and -independent ways

Lixia Lv[1], Guimin Zhao[1], Hongmei Wang*, Hongbin He*

Ruminant Disease Research Center, Key Laboratory of Animal Resistant Biology of Shandong, College of Life Science, Shandong Normal University, Shandong Province, China

ARTICLE INFO

Keywords:
Bovine parainfluenza virus type 3
Cholesterol 25-hydroxylase
25-hydroxycholesterol
Viral replication
Antiviral innate immunity

ABSTRACT

Bovine parainfluenza virus type 3 (BPIV3) is one of the most important pathogens associated with bovine respiratory diseases in both young and adult cattle widespreadly around the world. The host factors which participate in the infection of BPIV3 are poorly understood. Here, we found the bovine protein Cholesterol 25-hydroxylase (CH25 H) plays an important role in the infection of BPIV3. CH25H is a multi-transmembrane and endoplasmic reticulum-related enzyme that catalyzes oxidation reaction of cholesterol to production of 25-hydroxycholesterol (25HC) and significantly inhibits the replication of several viruses. In this study, we found that CH25H is an interferon-stimulated gene (ISG), which taken part in the antiviral innate immunity. In addition, the overexpression of CH25H could inhibit the replication of BPIV3, and 25HC significantly inhibited BPIV3 infection by preventing the synthesis of both virus antigenomic RNA (cRNA) and genomic RNA (gRNA) in MDBK cells. Interestingly, CH25H-M, a mutant lacking hydroxylase activity, still had an antiviral effect against BPIV3. Taken together, our findings highlight the antiviral function of CH25H during BPIV3 infection, and suggest that CH25H inhibits viral infection through both enzyme activity-dependent and -independent ways.

1. Introduction

Bovine parainfluenza virus type 3 (BPIV3), a member of the Paramyxoviridae family, can cause bovine respiratory diseases such as pneumonia and bronchopneumonia in both young and adult and widespread among cattle around the world (Murray et al., 2017; Zhao et al., 2018a, 2019). Epidemic outbreaks of these respiratory diseases could lead to an important health problem in the worldwide cattle (Headley et al., 2018). The BPIV3 genome is composed of negative-sense single-stranded RNA, approximately 15 kb in length, which encodes six structural proteins nuclear protein (NP or N), phosphoprotein (P), matrix protein (M), fusion protein (F), hemagglutinin neuraminidase protein (HN), large polymerase unit (L) and three non-structural proteins C, D and V proteins (Henrickson, 2003; Ellis, 2010). The genomic RNA (gRNA) acts as the template for the synthesis of messenger RNA (mRNA) and antigenomic RNA (cRNA) after the entry of virus particles, and the cRNA is the template for gRNA synthesis (Noton and Fearns, 2015). The virus will go through binding, fusion, uncoating, replication, budding and release of the virus to accomplish the viral infectious cycle (Moscona, 2005). Up to now, little is known about the regulatory mechanism of BPIV3 interaction with host cells. A better understanding of the pathogenic mechanisms of BPIV3 and the virus-host interactions in BPIV3 infection will facilitate development of more effective control measures.

Cholesterol-25-hydroxylase (CH25 H) is a 31.6-kDa multi-transmembrane and endoplasmic reticulum (ER)-associated enzyme that catalyzes the oxidation of cholesterol to produce 25-hydroxycholesterol (25HC) to reduce the accumulation of cholesterol (Holmes et al., 2011). 25HC, a natural oxysterol, controls sterol biosynthesis by regulating the sterol-responsive element binding protein (SREBP) and nuclear receptors activity (Blanc et al., 2013). CH25H and 25HC have been proved to play important roles in lipid metabolism and immune responses (Albers et al., 2006). It is known that the antiviral innate immune system is the first line of defense against pathogens infection (Rasmussen et al., 2009). Interferons (IFNs) are innate antiviral factors, which induce a strong antiviral effect through inducing the expression of interferon-stimulated genes (ISGs) (Schoggins and Rice, 2011). Previous studies have verified that CH25H is a classical ISG in murine macrophages and dendritic cells (Park and Scott, 2010). However, CH25H is not a classical ISG in human hepatocytes, and the up-regulation of CH25H is mediated by the innate immune adaptor molecules of MDA5, MAVS, IRF3, and NF-κB (Xiang et al., 2015). Recently,

* Corresponding authors: Present address: No. 88 Wenhua East Road, Lixia District, Jinan 250014, Shandong Province, China.
E-mail addresses: 15169049690@163.com (L. Lv), zgmnefu@163.com (G. Zhao), hongmeiwang@sdnu.edu.cn (H. Wang), hongbinhe@sdnu.edu.cn (H. He).
[1] The first two authors contributed equally to this work.

https://doi.org/10.1016/j.vetmic.2019.108456
Received 18 July 2019; Received in revised form 2 October 2019; Accepted 7 October 2019

CH25H has been identified as a major antiviral factor through producing 25HC, which has been shown to inhibit the infection of multiple viruses, including enveloped viruses (e.g. HCV (Anggakusuma et al., 2015; Chen et al., 2014), PRRSV (Ke et al., 2017; Song et al., 2019, 2017) and ZIKV (Li et al., 2017) and non-enveloped viruses (e.g. Poliovirus, Reovirus, HPV-16, HRoV and HRhV) (Lembo et al., 2016; Doms et al., 2018). Interestingly, CH25H-M, a mutant lacking hydroxylase activity, could also inhibit the infection of HCV, PRRSV, and PEDV by the mechanism independent of the hydroxylase activity of CH25H (Chen et al., 2014; Ke et al., 2017; Song et al., 2017; Zhang et al., 2019). However, the antiviral effects and mechanisms of CH25H and 25HC for paramyxovirus including BPIV3 remain unclear.

In the present study, we investigated the expression and antiviral role of CH25H during BPIV3 infection and found that CH25H is an ISG and plays a negtive role in the infection of BPIV3. The CH25H mRNA was up-regulated during BPIV3 infection, whereas the protein levels of CH25H were down-regulated in the later stages of BPIV3 infected MDBK cells and Hela cells. CH25H enzymatic activity product 25HC could inhibit BPIV3 replication in the phases of BPIV3 gRNA and cRNA synthesis in MDBK cells. And the CH25H-M still inhibited BPIV3 infection. These discoveries are helpful for the development of novel antiviral therapies against BPIV3 in the future.

2. Materials and methods

2.1. Cells and viruses

HEK 293 T cells and Hela cells were purchased from the Cell Bank of Type Culture Collection of the Chinese Academy of Sciences (Shanghai, China). Madin-Darby bovine kidney (MDBK) cells (CCL-22, ATCC) were preserved in our laboratory. All cells were propagated in DMEM (Invitrogen, Carlsbad, CA, USA) supplemented with 10% heat-inactivated fetal bovine serum (FBS) (Gibco, USA), penicillin (100 IU/mL), streptomycin (100 mg/mL) (Invitrogen) and incubated at 37 °C in a humidified incubator with 5% CO_2. A Chinese strain SD2014 of BPIV3 (No. CGMCC9992) obtained from China General Microbiological Culture Collection Center (CGMCC) (Yang et al., 2016). The 50% tissue culture infective dose ($TCID_{50}$) of BPIV3 was determined using the Reed-Müench method and was $1.0 \times 10^{6.6}$ $TCID_{50}$/0.1 mL.

2.2. Construction of plasmids

Bovine CH25H coding sequence (GenBank accession no. NM_001075243) was amplified by polymerase chain reaction (PCR) using the MDBK cells cDNA with the CH25H primer pair listed in Table 1. Then CH25H fragment was cloned into pEGFP-N1 vector (ClonTech, CA) to generate EGFP-tagged expression plasmid pEGFP-N1-CH25H. The histidine codons at positions 242 and 243 of wild-type bovine CH25H were converted to glutamine codons by site-directed mutagenesis to form CH25H-M. Then CH25H and CH25H-M fragments were subcloned into eukaryotic expression vector pLVX-IRES-puro (ClonTech, CA) with Flag-Tag at the N-terminus. The plasmids expressing HA-fusion proteins of BPIV3 or control plasmid were preserved in our laboratory. All constructed plasmids were confirmed by sequencing.

2.3. Plasmid transfection

HEK 293 T cells and Hela cells cultured in 6-well culture plates were transfected with recombinant plasmids expressing CH25H and CH25H-M using the Attractene Transfection Reagent (Qiagen, New York, USA) and Opti-MEM I (Gibco) according to the manufacturer's instructions. At 12 h post-transfection, the transfection mixture was replaced with the fresh medium and the cells were incubated at 37 °C in a humidified incubator containing 5% CO_2.

2.4. Western blot analysis

Cells were cultured in 6-well dishes and cleavaged with RIPA Lysis Buffer (Beyotime, China) plus 20 nM phenylmethylsulfonyl fluoride (PMSF). The protein samples were separated by SDS-PAGE and transferred to a polyvinylidene fluoride (PVDF) membrane (sc-3723, Santa Cruz, USA). Membranes were blocked with 5% skim milk in TBS-Tween (TBST) at room temperature for 2 h, and were probed with the appropriate primary antibodies at overnight at 4 °C. After washed three times with TBST, the membranes were incubated with the proper horseradish peroxidase (HRP)-conjugated secondary antibodies (Abcam, Cambridge, England) at room temperature for 1 h and then washed three times again with TBST. Protein band was visualized with the enhanced chemiluminescence (ECL) reagent (EpiZyme, Shanghai, China), using a chemiluminescence instrument (Tanon, Shanghai, China).

2.5. Generation of stable expression of CH25 H/CH25H-M gene MDBK cell lines

To package the recombinant lentiviruses expressing Flag-CH25H or Flag-CH25H-M, HEK 293 T cells were cotransfected with pLVX-Flag-CH25H-IRES-Puro or pLVX-Flag-CH25H-M-IRES-Puro and packaging vector pLP1, pLP2 and pLP-VSV-G (Invitrogen). The produced lentiviruses were harvested at 72 h post-cotransfection, filtered with a 45-μm filter, and infected MDBK cells for 48 h. Subsequently, the culture medium was replaced with fresh medium containing puromycin (Invitrogen) (2.2 μg/mL) every 2 to 3 days until puromycin-resistant colonies were obtained. Puromycin-resistant colonies were picked, and the expression of CH25 H/CH25H-M gene was detected with anti-Flag rabbit antibody (Cell Signaling Technology, USA) by western blot analysis.

2.6. RNA interference

To knockdown the expression of endogenous CH25H in MDBK cells (or Hela cells), the short hairpin RNAs (shRNAs) targeting CH25H were designed by web browser BLOCK-iT™ RNAi Designer, synthesized by TSINGKE Biological Technology Co., Ltd. (Beijing, China) and cloned into the pYr-Lvsh lentiviral vector. The sequences of shRNAs were listed in Table 1. HEK 293 T cells were cotransfected with pYr-Lvsh-CH25H and Lentivirus-assisted plasmids pLP1, pLP2 and pLP-VSV-G to package lentiviruses according to the manufacturer's instructions (Clontech, Palo Alto, CA). The supernatants containing shRNA-lentiviruses were harvested to infect MDBK cells (or Hela cells), and puromycin-resistant colonies were screened as described above. The knockdown efficiency of shRNA-mediated CH25H gene was detected with rabbit anti-CH25H (BIOSS, bs-23621R, China) and internal control β-actin (Cell Signaling Technology, USA) by western blotting. To investigate the effect of CH25H knockdown on the replication of BPIV3, MDBK (or HeLa) cell lines that stable knockdown of CH25H were infected with BPIV3 at an MOI of 0.1. At 24 h, 36 h (or 48 h) post-infection, the virus titers were detected.

2.7. Virus challenge and TCID50 assay for BPIV3

Hela or MDBK cell lines with expression CH25H or CH25H-M were plated into 6-well plates. Cells were infected with BPIV3 at a MOI of 0.1 for 24 h and 36 h or 48 h. The culture medium and cells were collected and repeated frozing and thawing for three times for virus titration to determine BPIV3 replication levels that expressed as the $\log_{10}TCID_{50}$/mL as previously described (Hou et al., 2019).

2.8. Real-time quantitative RT-PCR

Total RNA was extracted from cells using a Cell Total RNA Isolation

Table 1
List of primers used in this study

Primer name	Sequence (5'-3')	Application
CH25H-F-1	CACAAGATGCACCATCAGAATTC	qRT-PCR detection of CH25H (Bovine)
CH25H-R-1	CCCCGACGCTCATGTACTG	
CH25H-F-2	ACGTGGTCAACATCTGGCTTT	qRT-PCR detection of CH25H (Human)
CH25H-R-2	TGAGTGGACCAAGGGAAGTTGT	
IFN-β-F	CCTGTGCCTGATTTCATCATGA	qRT-PCR detection of IFN-β (Bovine)
IFN-β-R	GCAAGCTGTAGCTCCTGGAAAG	
ISG56-F-1	CAATCAGAAGTGAGAAGTCTGGTTACC	qRT-PCR detection of ISG56 (Bovine)
ISG56-R-1	TAAATCTGGGCTTCTGCCTGTT	
ISG56-F-2	AACACCCACTTCTGTCTTACTGCAT	qRT-PCR detection of ISG56 (Human)
ISG56-R-2	GATTTGGATCATTTGTGCCTTGT	
OAS1-F	GATGTCCTGCCCGCCTTT	qRT-PCR detection of OAS1 (Bovine)
OAS1-R	GCTGGACGTAGATTTGAGGGTTA	
IFITM3-F	CCTGACGACCACGGTGATC	qRT-PCR detection of IFITM3 (Bovine)
IFITM3-R	CAGGCAGCACCAGTTCATGA	
β-actin-F-1	GATGAGATTGGCATGGCTTTA	qRT-PCR detection of β-actin (Bovine)
β-actin-R-1	AACCGACTGCTGTCACCTTC	
β-actin-F-2	CGTGGACATCCGCAAAGAC	qRT-PCR detection of β-actin (Human)
β-actin-R-2	GCATCCTGTCGGCAATGC	
RT-gRNA	TGTTTGGAAATATGAATTTA	Specific chain reverse transcription
RT-cRNA	TTTGTTAGTTTAGTACCTAA	
BPIV3-F	AGAGAAGAGACTTGTTTGGAAATATGAA	qRT-PCR detection of BPIV3 gRNA and cRNA
BPIV3-R	CACTGAATGTATCAAACAGACTCAACAT	
N-F	TCTGGAGTTATGCAATGGGTG	qRT-PCR detection of BPIV3 N mRNA
N-R	CGTGCCACTGCTTGACCTA	
S-CH25H-1	CCCAAGCTTGCCACCATGAACAGCCACAACCGCTC	Construction of pEGFP-N1-CH25H
AS-CH25H-1	CGGGGATCCCGCTTGGCGTGAGCAGACCTCAG	
S-CH25H-2	CCGCTCGAG*GCCACCATGGACTACAAGGACGACGATGACAAG*AACAGCCACAACCGCTCCGA	Construction of pLVX-Flag-CH25H-IRES-Puro
AS-CH25H-2	CGGGGATCCTTACTTGGCGTGAGCAGACC	
S-CH25H-M	TCACGACCTG**CAGCAG**TCCCAGTTTAACTGCAAC	Construction of pLVX-Flag-CH25H-M-IRES-Puro
AS-CH25H-M	GA**CTGCTG**CAGGTCGTGATGCGCCACG	
shRNA1-CH25H-F-1	GATCCgcatctgctgcatcacaaggtCTCGAGACCTTGTGATGCAGCAGATGCTTTTTG	Construction of pYr-Lvsh-CH25H (bovine CH25H: 426-446)
shRNA1-CH25H-R-1	AATTCAAAAAGCATCTGCTGCATCACAAGGTCTCGAGCCTTGTGATGCAGCAGATGCG	Construction of pYr-Lvsh-CH25H (bovine CH25H: 723-743)
		Construction of pYr-Lvsh-CH25H (bovine CH25H: 743-763)
shRNA2-CH25H-F-1	GATCCgcatcactcccagtttaactgCTCGAGCAGTTAAACTGGGAGTGATGCTTTTTG	
shRNA2-CH25H-R-1	AATTCAAAAAGCATCACTCCCAGTTTAACTGCTCGAGCAGTTAAACTGGGAGTGATGCG	
shRNA3-CH25H-F-1	GATCCgcaactttgcgccttacttcaCTCGAGTGAAGTAAGGCGCAAAGTTGCTTTTTG	
shRNA3-CH25H-R-1	AATTCAAAAAGCAACTTTGCGCCTTACTTCACTCGAGTGAAGTAAGGCGCAAAGTTGCG	
shRNA1-CH25H-F-2	GATCCctcactttaactgcaacttCTCGAGAAGTTGCAGTTAAAGTGAGTTTTTG	Construction of pYr-Lvsh-CH25H (Human CH25H: 731-749)
shRNA1-CH25H-R-2	AATTCAAAAACTCACTTTAACTGCAACTTCTCGAGAAGTTGCAGTTAAAGTGAGG	Construction of pYr-Lvsh-CH25H (Human CH25H: 743-763)
shRNA2-CH25H-F-2	GATCCgcaacttcgctccgtactttaCTCGAGTAAAGTACGGAGCGAAGTTGC TTTTTG	
shRNA2-CH25H-R-2	AATTCAAAAAGCAACTTCGCTCCGTACTTTACTCGAG TAAAGTACGGAGCGAAGTTGCG	Construction of pYr-Lvsh-CH25H (Human CH25H: 396-416)
shRNA3-CH25H-F-2	GATCCgctactcttcgacatggagttCTCGAGAACTCCATGTCGAAGAGTAGC TTTTTG	
shRNA3-CH25H-R-2	AATTCAAAAAGCTACTCTTCGACATGGAGTTCTCGAGAACTCCATGTCGAAGAGTAGCG	
shNC-F	GATCCTTCTCCGAACGTGTCACGTCTCGAGACGTGACACGTTCGGAGAATTTTTG	Construction of negative control of shRNA
shNC-R	AATTCAAAAAACGTGACACGTTCGGAGAACTCGAGTTCTCCGAACGTGTCACGTG	

Notes: Underline, underline stands for the restriction endonuclease enzyme cutting sites; Italic, Flag-Tag sequence; Bold, mutation sites; lowercase, the position of shRNA targeting on CH25H gene.

Kit (Foregene, China) according to the manufacturer's instructions. Then RNA was reverse transcribed using a random primer RT kit (TaKaRa, Dalian, China). qRT-PCR analysis was performed in triplicate using SYBR Green PCR Master Mix (TaKaRa, Dalian, China) on a Light Cycler 480 II real-time PCR system (Roche, Germany) as previously reported (Hou et al., 2017, 2018a). Gene-specific primer sequences was designed by primer design software Primer Express 3.0, as shown in Table 1. The relative mRNA expression levels were quantified within each sample using the $2^{-\Delta\Delta Ct}$ method (Hou et al., 2018b), and β-actin mRNA expression levels were used as a house keeping gene for normalization process.

2.9. Viral attachment, internalization, replication and release assays

Attachment assay. MDBK cells were pre-treated with 25HC or ethanol at 37 °C for 12 h, followed by infecting cells with BPIV3 at 4 °C for 2 h. MDBK cells were washed three times with precooled PBS, the N mRNA levels of BPIV3 adsorbed on cells were measured using qRT-PCR. Internalization assays. MDBK cells were pre-treated with 25HC (15 μM) or ethanol at 37 °C for 12 h and then infected with BPIV3 (MOI of 1) at 4 °C. After 1 hpi, MDBK cells were washed with precooled PBS and incubated at 37 °C for another 2 h. BPIV3 N mRNA levels of internalized virus were measured by qRT-PCR. Replication assays. MDBK cells were pre-treated with 25HC (15 μM) or ethanol at 37 °C for 12 h and then infected with BPIV3 (MOI of 1) at 37 °C. At 8 hpi, the infected cells were collected to detect the gRNA, cRNA and mRNA levels of BPIV3 by qRT-PCR. Gene-specific primer sequences of BPIV3 gRNA, cRNA and mRNA was designed by primer design software Primer Express 3.0, as shown in Table 1. Strand-specific qRT-PCR to distinguish viral RNAs as previously described (Qiu et al., 2014). Release assays. MDBK cells were incubated with BPIV3 (MOI of 1). At 8 hpi, the virus-containing medium were replaced by fresh medium containing 25HC (15 μM) or ethanol. The medium were collected at 30, 60, and 90 min after treatment with 25HC and titrated by $TCID_{50}$ assays.

2.10. Statistical analyses

Statistical analyses were performed using GraphPad Prism 6.0 software (San Diego, CA, USA). Statistical significance was analyzed by two-way or one-way ANOVA multiple comparisons test that was made in grouped graphs or multiple samples. The results were presented as the mean values ± standard deviation (SD) from at least three independent experiments, and P value below 0.05 was considered statistically significant ($^{*}P < 0.05$; $^{**}P < 0.01$; $^{***}P < 0.001$; ns, not significant).

3. Results

3.1. The expression of CH25H gene is affected during BPIV3 infection

Previous studies have shown that the mRNA expression levels of CH25H could be rapidly induced by some viruses, such as ZIKV (Li et al., 2017) and HCV (Xiang et al., 2015). However, the expression of CH25H mRNA and protein was down-regulated in PRRSV-infected cells (Ke et al., 2017). To analyze the expression of CH25H in BPIV3 infected MDBK cells, the mRNA and protein levels of CH25H at different times during virus infection were detected by qRT-PCR and western blot assays. The results showed that CH25H mRNA (Fig. 1A) and protein (Fig. 1B) were dramatically up-regulated after BPIV3 infection, compared with the control groups in MDBK cells at 12 h and 24 h. However, BPIV3 infection significantly decreased CH25H protein expression in MDBK cells at 36 h (Fig. 1B). Next, we analyzed the expression of CH25H in BPIV3 infected Hela cells. An increased expression of CH25H mRNA was also observed in BPIV3 infected Hela cells at measured time points (Fig. 1C), whereas the decreased expression of CH25H protein was observed in BPIV3 infected Hela cells at later time points (24 h, 36 h and 48 h) (Fig. 1D). Taken together, these results demonstrated that the expression of CH25H mRNA was up-regulated by BPIV3 infection, whereas CH25H protein expression was down-regulated in the later stages of BPIV3 infected MDBK cells and Hela cells. Therefore, our results suggested that CH25H might has potential function in BPIV3 infection.

3.2. CH25H is an ISG in MDBK cells and Hela cells

CH25H was reported to be an ISG in murine macrophages and dendritic cells, but not in human hepatocytes (Park and Scott, 2010; Xiang et al., 2015). To verify whether CH25H is an ISG in MDBK cells and Hela cells, the cells were treated with poly (I:C) or IFN-β. The results showed that the mRNA levels of IFN-β, CH25H and ISG56 were significantly up-regulated after treatment with poly (I:C) (Fig. 2A). The mRNA levels of CH25H, OAS1, IFITM3 and ISG56 were also significantly up-regulated under IFN-β treatment (Fig. 2B). The expression of CH25H mRNA was also verified by qRT-PCR after the same treatment in Hela cells. As shown in Fig. 2**C and 2D**, the mRNA levels of IFN-β, CH25H, OAS1, IFITM3 and ISG56 were significantly induced under poly (I:C) or IFN-β treatment. Taken together, the results suggested that CH25H is an ISG in MDBK cells and Hela cells.

3.3. CH25H suppresses the replication of BPIV3

Previous studies have found that CH25H plays important roles in antiviral processes (Liu et al., 2013). The amino acid alignment of CH25H coding region from bovine were compared with human, murine and porcine CH25H and found that they have high sequence identities with bovine CH25H (**Figure. S1A**). In order to investigate whether bovine CH25H affected BPIV3 replication, the MDBK cell lines expressing Flag epitope-tagged CH25H (Flag-CH25 H) stably and empty plasmid vector (Flag-EV) were established. These cell lines were

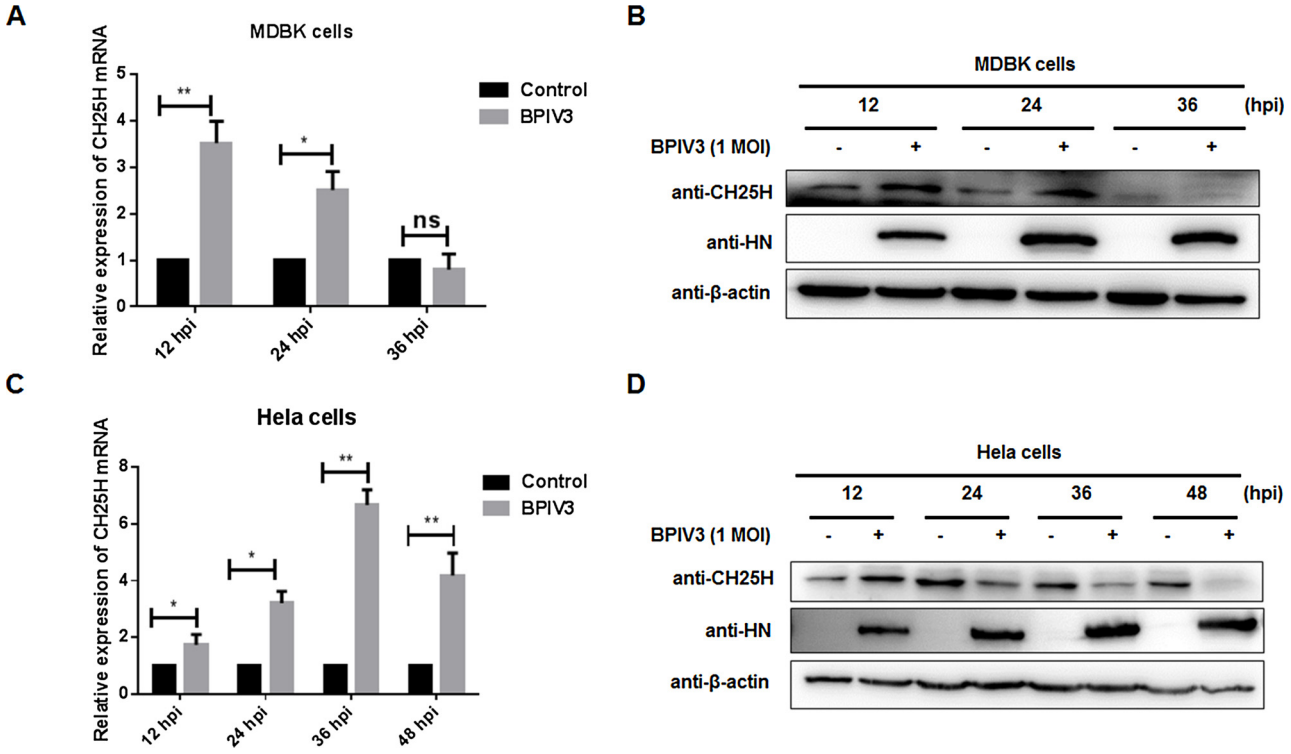

Fig. 1. CH25H gene expression is affected after BPIV3 infection.
MDBK or Hela cells were infected with BPIV3 (MOI of 1.0). At 12, 24 and 36 hpi, MDBK cells were harvested to detect the expression of CH25H mRNA by qRT-PCR **(A)** or the expression of CH25H protein by western blot analysis **(B)**. At 12, 24, 36 and 48 hpi, Hela cells were harvested to detect CH25H mRNA expression by qRT-PCR **(C)** or protein expression by western blot analysis **(D)**. The results depicted in panel A, C represent the means and standard deviations from three independent experiments. The results depicted in panel B and D are representatives of at least three biological repeats.

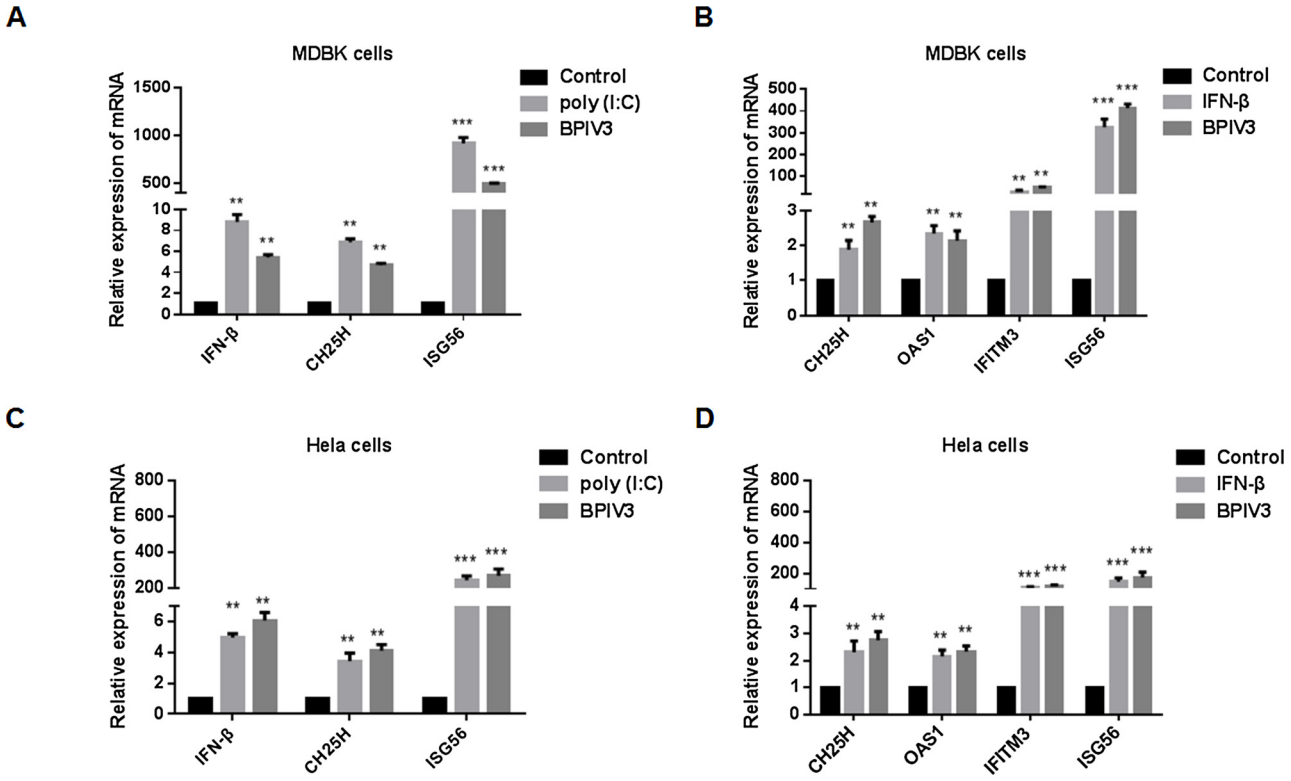

Fig. 2. CH25H is an ISG in MDBK cells and Hela cells.
(A) MDBK cells were transfected with poly (I:C) (2 μg/mL) (Invivogen, USA) and infected with BPIV3 (MOI of 1) for 12 h, cells were harvested to detect the mRNA levels of IFN-β, CH25H and ISG56 by qRT-PCR. **(B)** MDBK cells were stimulated with IFN-β (2.5×10^3 U/mL) (PeproTech, USA) and infected with BPIV3 (MOI of 2.5) for 2 h, cells were harvested to detect CH25H, OAS1, IFITM3, ISG56 mRNA expression by qRT-PCR. **(C)** Hela cells were transfected with poly (I:C) (2 μg/mL) and infected with BPIV3 (MOI of 1) for 12 h, cells were harvested to detect the mRNA levels of IFN-β, CH25H and ISG56 by qRT-PCR. **(D)** Hela cells were stimulated with IFN-β (2.5×10^3 U/mL) and infected with BPIV3 (MOI of 2.5) for 2 h, cells were harvested to detect CH25H, OAS1, IFITM3, ISG56 mRNA expression by qRT-PCR. The mean ± SD of the data were reported as three independent experiments.

infected with an equal amount of BPIV3 (MOI of 0.1) for 24 h and 36 h. BPIV3 HN protein and viral titers were determined to analyze whether CH25H affected the replication of BPIV3. As shown in Fig. 3**A and B**, CH25H significantly inhibited the replication of BPIV3 at measured time points. Next, bovine CH25H gene was ectopically overexpressed in Hela cells. Here, we found that the BPIV3 HN protein (Fig. 3C) and virus titers (Fig. 3D) were significantly reduced in overexpressed CH25H cells compared with control cells transfected with pEGFP-N1 at 24 hpi and 48 hpi.

To further explore the effect of CH25H on BPIV3 replication, the shRNAs targeting bovine CH25H and human CH25H were designed, respectively. And then, stable knockdown of CH25H gene by shRNA lentivirus mediated MDBK and Hela cell lines, as well as their corresponding negative control cell lines were constructed. The interference efficiencies of CH25H in shRNA-mediated knockdown cell lines were examined by western blot analysis. As shown in Fig. 4A, the three shRNAs exhibited varied knockdown effects on CH25H expression in MDBK cell lines, and the highest efficient shRNA3-CH25H was used in the following experiments. Subsequently, shRNA-mediated CH25H knockdown MDBK cell lines were infected with BPIV3 for 24 h and 36 h, and viral titers were determined to testify whether knockdown CH25H affected the replication of BPIV3. As shown in Fig. 4B, knockdown of CH25H promoted the replication of BPIV3 compared with the negative control. The same experiments were performed in Hela cells. As shown in Fig. 4C, among the three shRNA-mediated CH25H knockdown Hela cell lines, shRNA1-CH25H is the most efficient. Similarly, knockdown of CH25H promoted BPIV3 replication (Fig. 4D). Collectively, the results suggested that overexpression of CH25H significantly inhibited BPIV3 replication, and knockdown of CH25H promoted the infection of BPIV3.

3.4. 25HC inhibits the synthesis of BPIV3 cRNA and gRNA in MDBK cells

To investigate whether the inhibition of CH25H on BPIV3 replication is dependent on its enzymatic activity, we first verified the cytotoxicity of 25HC to MDBK cells. We found that 25HC at concentrations as high as 15 μM showed no obvious cytoxicity to MDBK cells (Fig. 5A). Next, MDBK cells were pre-treated with different concentrations of 25HC (5, 10 and 15 μM) (Sigma, USA) for 12 h and then infected with BPIV3 (MOI of 0.1). After infection for 24 h, virus titers were measured by $TCID_{50}$ assays. As illustrated in Fig. 5B, treatment with 25HC significantly inhibited BPIV3 replication in a dose-dependent manner without obvious cytotoxicity to MDBK cells.

To further investigate the mechanism by which 25HC inhibits BPIV3 infection, the BPIV3 growth curve was determined firstly. The RNA of BPIV3 N gene from the BPIV3 infected MDBK cells were measured by qRT-PCR, and virus titer was measured by $TCID_{50}$ assays. The specific time points of BPIV3 infectious cycle were determined. As shown in Fig. 5**C and D**, BPIV3 genome replication was performed at 4 th and release at 8 th hour in infected MDBK cells, respectively. Next, we explored which stage of the BPIV3 life cycle was inhibited by 25HC. The RNA levels and virus titers of BPIV3 were measured by qRT-PCR and $TCID_{50}$ assays at the corresponding stage of virus replication, respectively. The results, depicted in Fig. 5**E and F**, 25HC inhibited the replication of BPIV3 by inhibiting the synthesis of BPIV3 cRNA and gRNA in MDBK cells. Taken together, these results indicated that 25HC was a potent agent against BPIV3 infection at the replication stage.

3.5. CH25H-M could also suppress the infection of BPIV3

It has been reported that the clustered histidines residues of CH25H

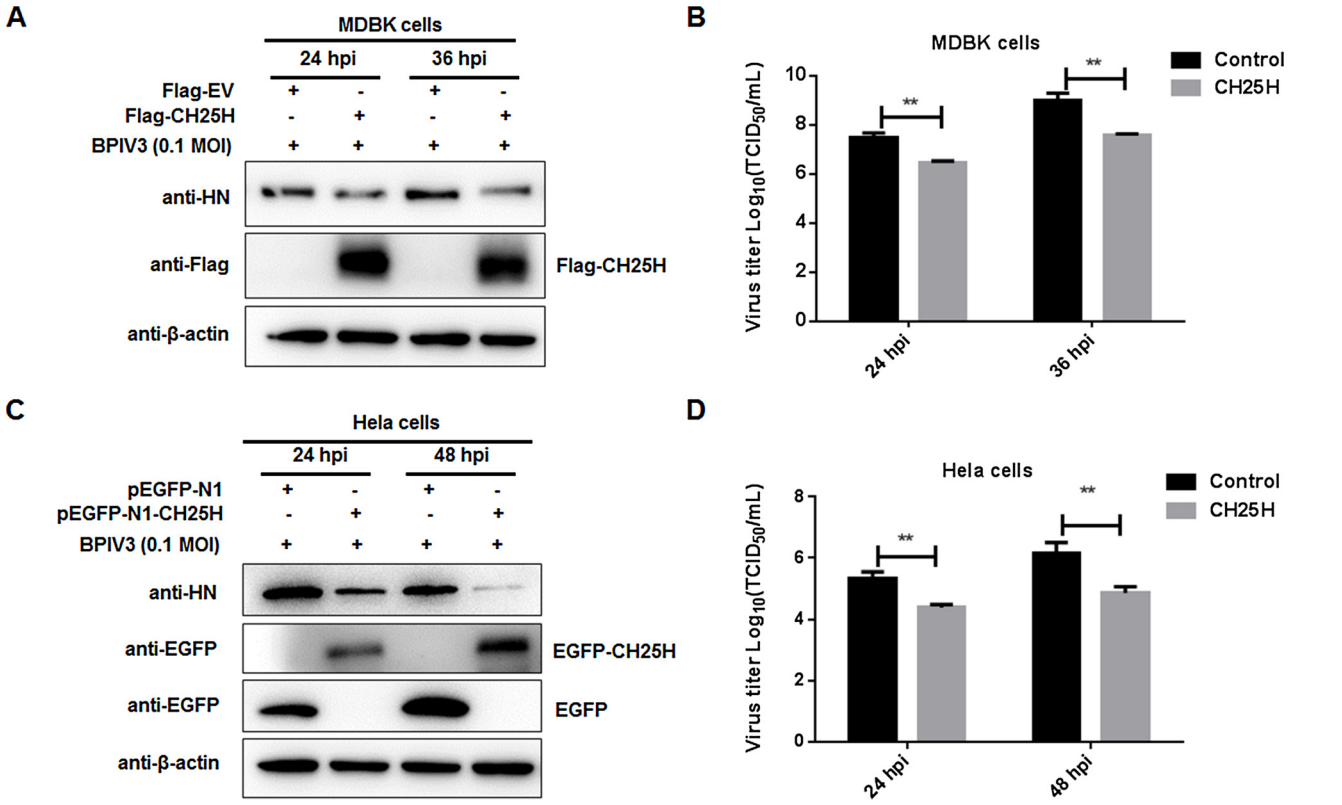

Fig. 3. Overexpression of CH25H inhibits BPIV3 replication.
MDBK cell lines that stably overexpressing CH25H were infected with BPIV3 (MOI of 0.1). At 24 and 36 hpi, cells were harvested to analyze CH25H and BPIV3 HN expression by western blot analysis with the anti-CH25H monoclonal antibody and anti-HN polyclonal antibody (Ruminant Disease Research Center of Shandong normal University, China) **(A)**, and the culture medium and cells were harvested to analyze virus titers by $TCID_{50}$ assays **(B)**. Hela cells were transfected with pEGFP-N1-CH25H or control pEGFP-N1. After 24 h transfection, cells were infected with BPIV3 (MOI of 0.1). At 24 and 48 hpi, cells were harvested to analyze CH25H and BPIV3 HN protein expression by western blot analysis **(C)**, and the culture medium and cells were harvested to analyze virus titers by $TCID_{50}$ assays **(D)**. The results depicted in panel A and C are representatives of at least three biological repeats. The results depicted in panel B and D are expressed as means and standard deviations from three independent experiments.

are critical for its enzymatic activity (Lund et al., 1998). To investigate whether the enzymatic activity of CH25H is indispensable for the antiviral activity of CH25H against BPIV3, the bovine CH25H-M with 242 and 243 histidine residues substituted by glutamine was constructed by site-directed mutagenesis (Fig. 6A). The lentivirus-mediated overexpression of CH25H-M was used to research the antiviral effect of CH25H-M on BPIV3 in MDBK cells. Firstly, we verified the expression of CH25H-M in MDBK cells by western blot analysis. As shown in Fig. 6B, the expression of CH25H-M-3 was the highest. Next, the expression of BPIV3 HN protein was analyzed by western blot and virus titers were determined by $TCID_{50}$ assays in MDBK cell lines overexpressing CH25H and CH25H-M. The results showed that CH25H-M significantly inhibited the expression of BPIV3 HN protein at 24 h and viral titer at 36 h by approximately 8-fold relative to that of control group, whereas the antiviral effects of CH25H-M were less than that of wild type CH25H (Fig. 6**C and D**). These results indicated that the antiviral functions of CH25H on BPIV3 was not entirely dependent on its enzymatic activity.

3.6. BPIV3 down-regulates the expression of CH25H protein by impairing the stability of CH25H in Hela cells

The ubiquitin-proteasome system, autophagy and apoptosis are three major pathways of intracellular protein degradation in eukaryotic cells (Schreiner et al., 2012; Wang et al., 2019). In order to verify the down-regulation of CH25H protein expression by which pathway, the autophagy inhibitor CQ, the apoptosis inhibitor Z-VAD-FMK and the proteasome inhibitor MG132 were added to Hela cells infected with BPIV3. We found that the down-regulated expression of CH25H protein was not affected by treatment with MG132, CQ (Fig. 7A) and Z-VAD-FMK (Fig. 7B). Then, we verified whether viral proteins affect the expression of CH25H protein. The results showed that the overexpression of viral proteins had no effect on CH25H protein (Fig. 7C). Next, we further verified whether BPIV3 infection had an impact on the stability of CH25H protein. As shown in Fig. 7D, BPIV3 infection promoted the degradation of CH25H in the presence of CHX. In sum, these results indicated that BPIV3 infection reduced the stability of CH25H protein, thereby the protein levels of CH25H were down-regulated in the later stages of BPIV3 infection.

4. Discussion

As one of the most important respiratory pathogens of cattle, BPIV3 has devastated the cattle industry worldwidely for several decades (Leal et al., 2019; Zhao et al., 2018b). Although many commercial vaccines have been produced to prevent BPIV3 infection, unfortunately, current preventive and control strategies can not provide sustainable control in cattle infected with BPIV3. In recent years, host antiviral restriction factors have received more and more attention (Liu et al., 2013). The study of host antiviral factors will help us to better understand the mechanism against viral infection and facilitate the development of novel vaccines and antiviral drugs. CH25H has recently been identified as a host restriction factor that inhibits the replication of many viruses by catalyzing the production of 25HC (Xiang et al., 2015). In this study, we found that CH25H plays an antiviral role in BPIV3 infection.

Cholesterol is an important component of cellular membranes and is

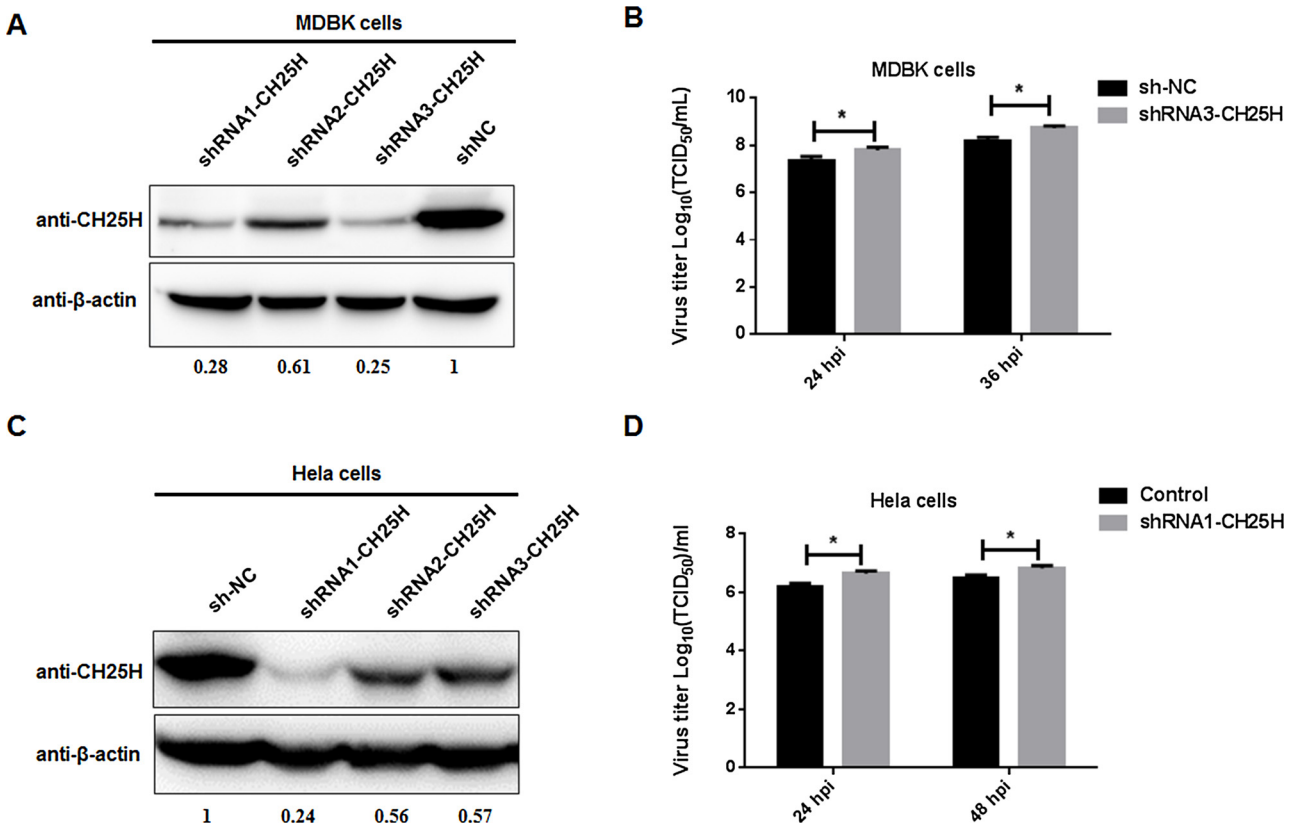

Fig. 4. Knockdown of CH25H promotes the replication of BPIV3.
(A) The knockdown efficiencies of CH25H-shRNA in stable MDBK cell lines were assayed by western blotting with anti-CH25H antibody. **(B)** shRNA3-mediated knockdown MDBK cell lines shRNA3-CH25H and their corresponding control groups were infection with BPIV3 (MOI of 0.1) for 24 h and 36 h, then the titers of BPIV3 infected cells were determined by $TCID_{50}$ assays. **(C)** The knockdown efficiencies of CH25H-shRNA in stable Hela cell lines were assayed by western blotting with anti-CH25H antibody. **(D)** shRNA1-mediated knockdown Hela cell lines shRNA1-CH25H and their corresponding control groups were infection with BPIV3 (MOI of 0.1) for 24 h and 48 h, then the titers of BPIV3 infected cells were determined by $TCID_{50}$ assays. The results depicted in panel A, C are representatives of at least three biological repeats. The results depicted in panel B, D are expressed as means and standard deviations from three independent experiments.

crucial to a broad range of cellular functions. It is known that the homeostatic pathways and natural immune response that control cellular cholesterol metabolism are mutually regulated (Yvan-Charvet et al., 2019). CH25H is an enzyme that converts oxidation of cholesterol to 25HC, which regulates cholesterol and lipid metabolism. Recent studies have found that 25HC exerts its antiviral affects by multiple mechanisms. In 2016, David Lembo and colleagues summarized broad spectrum antiviral activity of 25HC against the enveloped viruses and non-enveloped (Lembo et al., 2016). For example, 25HC restricts the infection of ZIKV, PRRSV and PEDV by inhibiting viral penetration (Li et al., 2017; Ke et al., 2017; Song et al., 2019; Zhang et al., 2019); 25HC inhibits HCV replication by preventing the formation of membranous web (Anggakusuma et al., 2015); 25HC blocks a post entry stage of MCMV replicative cycle (Blanc et al., 2013); 25HC was also reported to repress HCV infection at the postentry step by suppressing the activation of SREBP2 (Xiang et al., 2015); 25HC exerts its antiviral effect by inhibiting the glycosylation of the glycoprotein GP1 of Lassa fever virus (LASV) (Shrivastava-Ranjan et al., 2016). In addition, 25HC has also significant antiviral activity against non-enveloped viruses. For example, 25HC suppresses Poliovirus (PV) replication by reducing the production and accumulation of PI4P at the Golgi complex by targeting oxysterol binding protein (OSBP) family I in PV-infected cells (Arita et al., 2013). Treatment with 25HC alters transport of mammalian *orthoreovirus* (reovirus) particles to late endosomes and delays the uncoating of reovirus, thereby inhibiting the efficiency of cellular entry of reovirus (Doms et al., 2018). In our study, overexpression of CH25H significantly inhibited the replication of BPIV3 in MDBK cells and Hela cells. Judging from the results of the decrease of BPIV3 HN protein and titer in MDBK cells overexpressing CH25H, approximately 10-fold higher anti-virus effects of CH25H compared to control groups. And, knockdown of CH25H gene by shRNA promoted the replication of BPIV3 in MDBK cells and Hela cells. Because the sequence of bovine CH25H is different from that from human CH25H, the position of each shRNA targeting on both bovine and human CH25H gene is different. Therefore, the silencing efficiency and the antiviral effect of different shRNA-CH25H in different cells are also different. Next, we investigated the antiviral potency of CH25H enzymatic activity product 25HC on BPIV3 infection. We elucidated that 25HC restricted BPIV3 infection at a postentry step, which is similar to the inhibition mechanism of 25HC against HCV and MCMV (Xiang et al., 2015; Blanc et al., 2013). The replication of negative-sense single-stranded RNA viruses in cells is different from other viruses. The replication of BPIV3 genome in cells include the synthesis of cRNA and gRNA. In this study, we found that exogenous treatment of 25HC inhibited BPIV3 cRNA and gRNA synthesis in MDBK cells.

Beyond that, recent studies demonstrate that CH25H also inhibits viral replication by enzymatic activity-independent pathways. For instance, CH25 H/CH25H-M could suppress PRRSV replication by degrading the nonstructural protein 1 alpha (nsp1α) of PRRSV through the ubiquitin-proteasome pathway (Ke et al., 2017). CH25H restricts HCV replication through inhibiting HCV NS5A dimer formation (Chen et al., 2014). In this study, we also showed that another antiviral effect employed by CH25H to inhibit BPIV3 infection that is independent of its enzymatic activity. However, in the study of the antiviral mechanism of CH25H-M, we verified that there was no direct interaction between BPIV3 protein and CH25H protein using yeast two-hybrid system

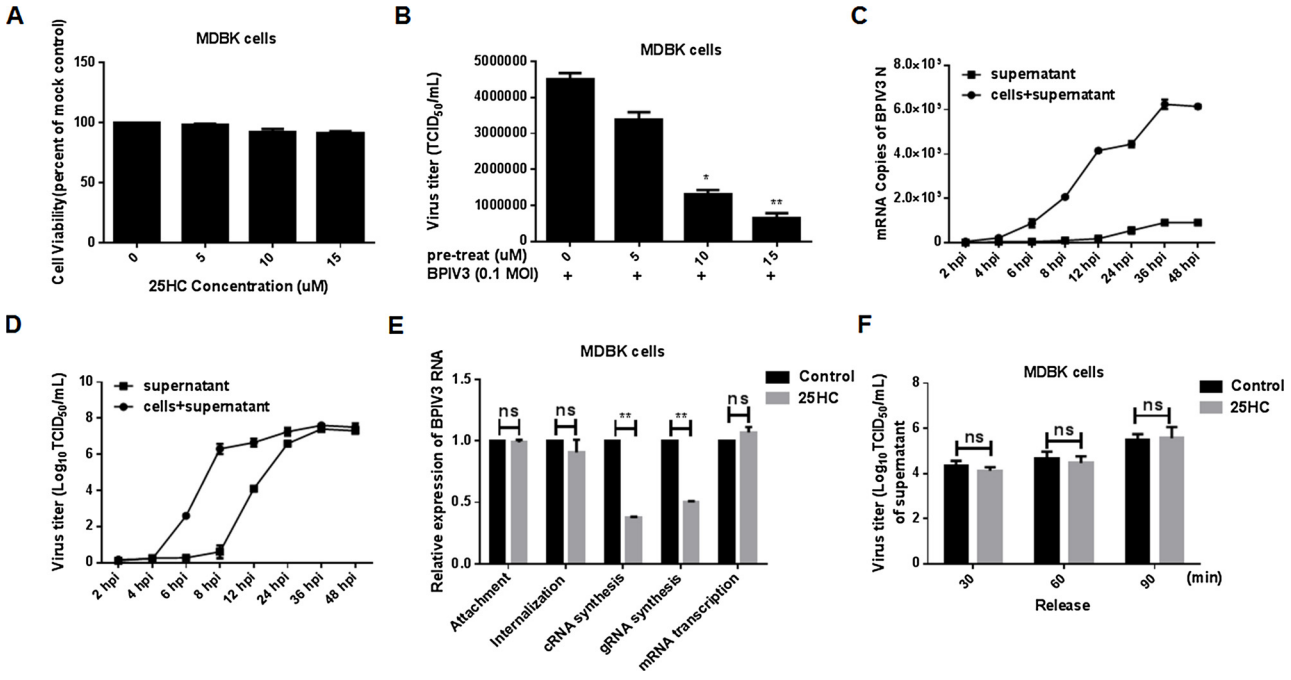

Fig. 5. 25HC inhibits BPIV3 cRNA and gRNA synthesis.
(A) Different concentrations of 25HC (5, 10, and 15 μM) were added to MDBK cells incubated for 48 h in 96-well dishes. Cell viability then was determined by an MTT assay according to the manufacturer's instructions (Sigma, USA). **(B)** MDBK cells were pre-treated with 25HC (5, 10 and 15 μM) at the different concentrations for 12 h prior to BPIV3 infection (MOI of 0.1), the culture medium and cells were harvested for the $TCID_{50}$ assays at 24 hpi. MDBK cells were infected with BPIV3 (MOI of 1). After incubation for 2 h, 4 h, 6 h, 8 h, 12 h, 24 h, 36 h and 48 h, cells or supernatant were collected to detect N gene mRNA of BPIV3 by qRT-PCR **(C)**, and the culture medium or cells were collected to detect virus titers by $TCID_{50}$ assays **(D)**. **(E)** Attachment assay. MDBK cells were pre-treated with 25HC (15 μM) or ethanol at 37 °C for 12 h, followed by infecting cells with BPIV3 (MOI of 1) at 4 °C. After incubation for 2 h, MDBK cells were washed three times with precooled PBS, and then cell lysates were prepared, BPIV3 N mRNA levels were measured using qRT-PCR. Internalization assays. MDBK cells were pre-treated with 25HC (15 μM) or ethanol at 37 °C for 12 h and then infected with BPIV3 (MOI of 1) at 4 °C for 1 h. MDBK Cells were washed with precooled PBS and incubated at 37 °C for another 2 h. BPIV3 N mRNA levels of internalized virus were measured by qRT-PCR. Replication assays. MDBK cells were pre-treated with 25HC (15 μM) or ethanol at 37 °C for 12 h and then infected with BPIV3 (MOI of 1) at 37 °C. At 8 hpi, the infected cells were collected to detect the gRNA, cRNA and mRNA levels of BPIV3 by qRT-PCR. **(F)** Release assays. MDBK cells were incubated with BPIV3 (MOI of 1). At 8 hpi, the virus-containing medium were replaced by fresh medium containing 25HC (15 μM) or ethanol. The medium were collected at 30, 60, and 90 min after treatment with 25HC and titrated by $TCID_{50}$ assays. Data were expressed as means and standard deviations from three independent experiments.

(**Figure. S2A**). Furthermore, the study of antiviral mechanism of CH25H-M is the major task in the future.

It has been reported that the expression levels of CH25H gene are low to undetectable in many tissues and cells *in vivo*. When IFNs signaling pathway is activated by various toll-like receptor (TLR) ligands and IFN molecules, the CH25H gene is rapidly expressed in many tissues such as liver, heart, brain, muscle, kidney and lung (Park and Scott, 2010). In most cells, viral infection triggers the production of IFNs that then bind to receptors on nearby cells and induce a forceful transcriptional program including hundreds of antiviral ISGs (Schneider et al., 2014). The expression of CH25H is different in response to different viral infections. Previous studies have indicated that the expression of CH25H is up-regulated during HCV (Anggakusuma et al., 2015), ZIKV (Li et al., 2017) and MCMV (Blanc et al., 2013) infection; as opposed to this, CH25H is reduced in response to HSV-1 (You et al., 2017), PRRSV (Ke et al., 2017) and PEDV infection (Zhang et al., 2019). Whether it is related to the dose or the specificity of the virus needs to be further explored. Here, we found that CH25H mRNA was dramatically induced by type I IFN and BPIV3 infection, and CH25H is an ISG in MDBK cells and Hela cells. However, the expression of CH25H protein was significantly decreased in the later stages of BPIV3 infected MDBK cells and Hela cells. However, very few reports actually looked into the changes within the protein levels of CH25H following virus infection. Dong et al. (2018) found that the nonstructural protein 1β and nsp11 of PRRSV degraded CH25H protein by lysosomal pathway in HEK 293FT cells. After further research, we found that BPIV3 infection reduced the stability of CH25H protein, whereas the expression of CH25H was not restored by treatment with MG132, CQ, or Z-VAD-FMK. Previous studies have revealed that the paramyxovirus P gene encodes accessory proteins C and V antagonistic to IFN (Eberle et al., 2015; Komatsu et al., 2007). Therefore, whether these IFN antagonists are involved in BPIV3-induced down-regulation of CH25H is a subject of future research.

5. Conclusions

In summary, our studies demonstrated that CH25H possessed antiviral activity against BPIV3 for the first time. These findings indicated that CH25H was able to suppress BPIV3 infection through both 25HC-dependent and independent ways, which potentially provides a new view on the therapies of BPIV3 (Fig. 8). Further studies are assuring to more accurately elucidate the antiviral mechanisms of CH25H-M on BPIV3 infection and the significance of BPIV3-induced down-regulation of CH25H protein.

6. Competing interests

The authors declared no potential conflicts of interest with respect to the research, authorship, and/or publication of this article.

7. Authors' contributions

L.LX and Z.GM performed the experiments and drafted manuscript, H.HB and W.HM designed and instructed the experiments. All authors have read and approved the final manuscript.

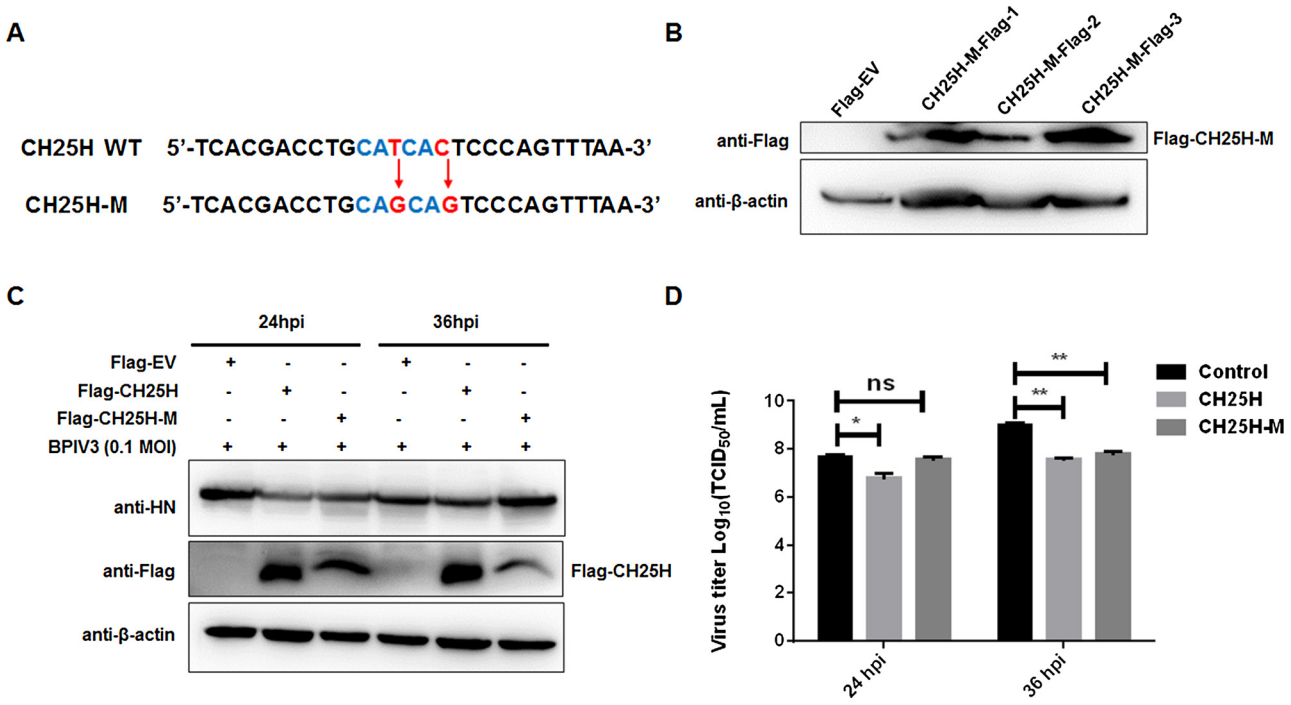

Fig. 6. CH25H-M lacking hydroxylase activity can inhibit BPIV3 replication.
(A) To create a CH25H catalytic mutant form (CH25H-M), histidine codons at positions 242 and 243 of bovine wild-type CH25H were converted to glutamine codons by site-directed mutagenesis. **(B)** The MDBK cells lines expressing recombinant lentivirus pLVX-CH25H-M-Flag-IRES-Puro or expressing control lentivirus pLVX-Flag-IRES-Puro were harvested to determine CH25H-M expression by western blot assay. MDBK stable cell lines of overexpressing CH25H and CH25H-M were infected with BPIV3 (MOI of 0.1). At 24 and 36 hpi, cells were harvested to detect BPIV3 HN protein by western blot **(C)**, and the culture medium and cells were collected to detect virus titers by $TCID_{50}$ assays **(D)**. All the results were confirmed by three independent experiments. The mean ± SD of the data represent the standard deviations of triplicate experiments.

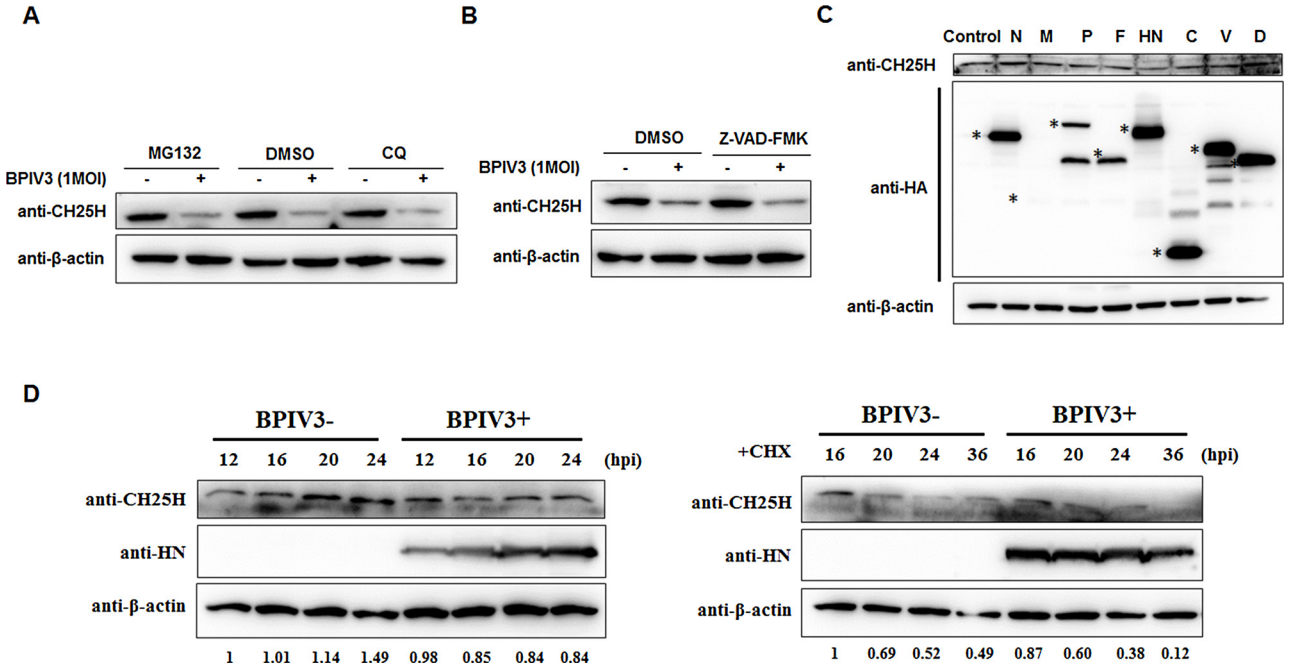

Fig. 7. CH25H protein stability is impaired at the later stages of BPIV3 infection.
(A-B) Hela cells were pre-treated with the proteasome inhibitor MG132 (10 μM) (MedChemExpress, USA), the autophagy inhibitors CQ (20 μM) (Sigma, USA), and the apoptosis inhibitor Z-VAD-FMK (10 μM) (MedChemExpress, USA) for 4 h and then infected with 1.0 MOI of BPIV3. At 24 hpi, the levels of the CH25H, p62, C-Caspase3 and C-PARP protein were determined by western blotting with the anti-CH25H, anti-p62 (Cell Signaling Technology, USA), anti-C-Caspase3 (Cell Signaling Technology, USA) and anti-C-PARP (Cell Signaling Technology, USA) monoclonal antibodies. **(C)** Hela cells were transfected with the plasmids expressing HA-fusion proteins of BPIV3 or control plasmid (1.2 μg). The cells lysates at 48 h post-transfection were collected and subjected to western blot analysis with anti-CH25H, anti-HA (Cell Signaling Technology, USA) and anti-β-actin antibody. **(D)** Hela cells were infected and mock-infection with BPIV3 (MOI of 1.0), and then treated with CHX (100 μM) (MedChemExpress, USA) at 12 h post-infection. Cells were harvested to detect the protein expression of CH25H at various time by western blot analysis. All the results were confirmed by three independent experiments. C-Caspase3, Cleaved-Caspase3; C-PARP, Cleaved-PARP.

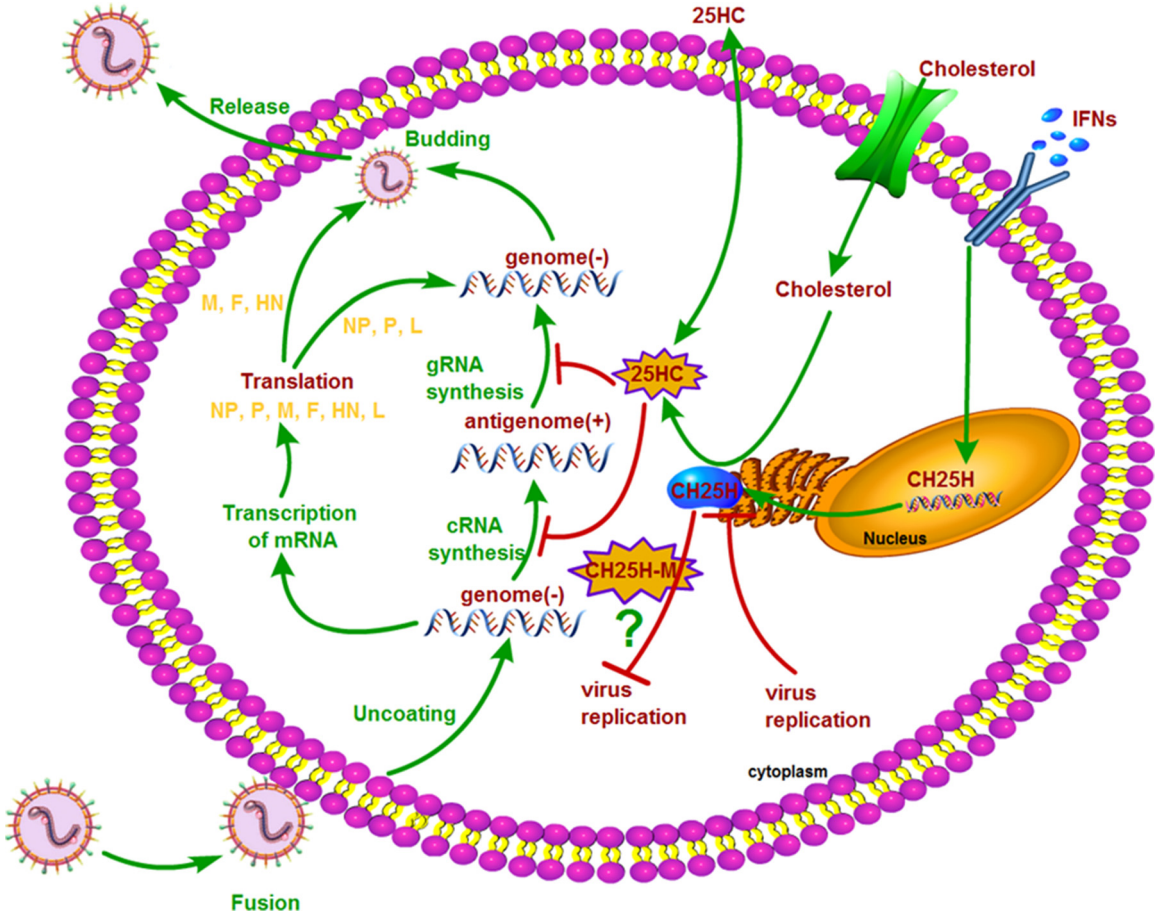

Fig. 8. A proposed mechanism underlying CH25H inhibits BPIV3 replication.
The model showed the antiviral effect of an ISG, IFN-induced CH25H to control BPIV3 replication by inhibiting virus cRNA and gRNA synthesis in MDBK cells. BPIV3 induced the production of a large number of IFNs, and then IFNs triggered the production of CH25H by activating the IFN signaling pathway. CH25H catalyzed oxidation of cholesterol to 25HC and significantly inhibited cRNA and gRNA synthesis of BPIV3. CH25H-M that lacking hydroxylase activity still suppressed BPIV3 infection, whereas the antiviral mechanism of CH25H-M on BPIV3 remains unclear. And BPIV3 inhibited the expression of CH25H in the later stages of BPIV3 infected cells in order to facilitate its own replication.

Acknowledgments

We thank Dr. Xiaopeng Zhang for modifying the manuscript. This work was partly supported by grants from the National Natural Sciences Foundation of China (31872490), National Primary Research & Development Plan (2018YFD0501600), Primary Research & Development Plan of Shandong Province (2018GNC113011) and the earmarked fund for the Taishan Scholar Project (Hongbin He).

Appendix A. Supplementary data

Supplementary material related to this article can be found, in the online version, at doi:https://doi.org/10.1016/j.vetmic.2019.108456.

References

Albers, M., Blume, B., Schlueter, T., Wright, M.B., Kober, I., Kremoser, C., Deuschle, U., Koegl, M., 2006. A novel principle for partial agonism of liver X receptor ligands. Competitive recruitment of activators and repressors. J. Biol chem. 281 (8), 4920–4930.

Anggakusuma, Romero-Brey, I., Berger, C., Colpitts, C.C., Boldanova, T., Engelmann, M., Todt, D., Perin, P.M., Behrendt, P., Vondran, F.W., Xu, S., Goffinet, C., Schang, L.M., Heim, M.H., Bartenschlager, R., Pietschmann, T., Steinmann, E., 2015. Interferon-inducible cholesterol-25-hydroxylase restricts hepatitis C virus replication through blockage of membranous web formation. Hepatology. 62 (3), 702–714.

Arita, M., Kojima, H., Nagano, T., Okabe, T., Wakita, T., Shimizu, H., 2013. Oxysterol-binding protein family I is the target of minor enviroxime-like compounds. J. Virol. 87, 4252–4260.

Blanc, M., Hsieh, W.Y., Robertson, K.A., Kropp, K.A., Forster, T., Shui, G., Lacaze, P., Watterson, S., Griffiths, S.J., Spann, N.J., Meljon, A., Talbot, S., Krishnan, K., Covey, D.F., Wenk, M.R., Craigon, M., Ruzsics, Z., Haas, J., Angulo, A., Griffiths, W.J., Glass, C.K., Wang, Y., Ghazal, P., 2013. The transcription factor STAT-1 couples macrophage synthesis of 25-hydroxycholesterol to the interferon antiviral response. Immunity 38 (1), 106–118.

Chen, Y., Wang, S., Yi, Z., Tian, H., Aliyari, R., Li, Y., Chen, G., Liu, P., Zhong, J., Chen, X., Du, P., Su, L., Qin, F.X., Deng, H., Cheng, G., 2014. Interferon-inducible cholesterol-25-hydroxylase inhibits hepatitis C virus replication via distinct mechanisms. Sci. Rep. 4, 7242.

Doms, A., Sanabria, T., Hansen, J.N., Altan-Bonnet, N., Holm, G.H., 2018. 25-Hydroxycholesterol Production by the Cholesterol-25-Hydroxylase Interferon-Stimulated Gene Restricts Mammalian Reovirus Infection. J. Virol. 92 (18).

Dong, H., Zhou, L., Ge, X., Guo, X., Han, J., Yang, H., 2018. Porcine reproductive and respiratory syndrome virus nsp1β and nsp11 antagonize the antiviral activity of cholesterol-25-hydroxylase via lysosomal degradation. Vet. Microbiol. 223, 134–143.

Eberle, K.C., McGill, J.L., Reinhardt, T.A., Sacco, R.E., 2015. Parainfluenza Virus 3 Blocks Antiviral Mediators Downstream of the Interferon Lambda Receptor by Modulating Stat1 Phosphorylation. J. Virol. 90 (6), 2948–2958.

Ellis, J.A., 2010. Bovine parainfluenza-3 virus. Vet Clin North Am Food Anim Pract. 26 (3), 575–593.

Headley, S.A., Okano, W., Balbo, L.C., Marcasso, R.A., Oliveira, T.E., Alfieri, A.F., Negri Filho, L.C., Michelazzo, M.Z., Rodrigues, S.C., Baptista, A.L., Saut, J.P.E., Alfieri, A.A., 2018. Molecular survey of infectious agents associated with bovine respiratory disease in a beef cattle feedlot in southern Brazil. J. Vet. Diagn Invest. 30 (2), 249–251.

Henrickson, K.J., 2003. Parainfluenza viruses. Clin Microbiol Rev. 16 (2), 242–264.

Holmes, R.S., Vandeberg, J.L., Cox, L.A., 2011. Genomics and proteomics of vertebrate cholesterol ester lipase (LIPA) and cholesterol 25-hydroxylase (CH25H). 3 Biotech. 1 (2), 99–109.

Hou, P., Wang, H., Zhao, G., He, C., He, H., 2017. Rapid detection of infectious bovine Rhinotracheitis virus using recombinase polymerase amplification assays. BMC Vet. Res. 13, 386.

Hou, P., Zhao, G., Wang, H., He, C., He, H., 2018a. Rapid detection of bovine viral

diarrhea virus using recombinase polymerase amplification combined with lateral flow dipstick assays in bulk milk. Vet. Arhiv. 88 (5), 627–642.
Hou, P., Zhao, G., He, C., Wang, H., He, H., 2018b. Biopanning of polypeptides binding to bovine ephemeral fever virus G1 protein from phage display peptide library. BMC Vet. Res. 14 (1), 3.
Hou, P., Zhao, M., He, W., He, H., Wang, H., 2019. Cellular microRNA bta-miR-2361 inhibits bovine herpesvirus 1 replication by directly targeting EGR1 gene. Vet. Microbiol. 233, 174–183.
Ke, W., Fang, L., Jing, H., Tao, R., Wang, T., Li, Y., Long, S., Wang, D., Xiao, S., 2017. Cholesterol 25-Hydroxylase Inhibits Porcine Reproductive and Respiratory Syndrome Virus Replication through Enzyme Activity-Dependent and -Independent Mechanisms. J. Virol. 91 (19).
Komatsu, T., Takeuchi, K., Gotoh, B., 2007. Bovine parainfluenza virus type 3 accessory proteins that suppress beta interferon production. Microbes and infection 9 (8), 954–962.
Lembo, D., Cagno, V., Civra, A., Poli, G., 2016. Oxysterols: An emerging class of broad spectrum antiviral effectors. Mol. Aspects Med. 49, 23–30.
Leal, E., Liu, C., Zhao, Z., Deng, Y., Villanova, F., Liang, L., Li, J., Cui, S., 2019. Isolation of a Divergent Strain of Bovine Parainfluenza Virus Type 3 (BPIV3) Infecting Cattle in China. Viruses. 11 (6).
Li, C., Deng, Y.Q., Wang, S., Ma, F., Aliyari, R., Huang, X.Y., Zhang, N.N., Watanabe, M., Dong, H.L., Liu, P., Li, X.F., Ye, Q., Tian, M., Hong, S., Fan, J., Zhao, H., Li, L., Vishlaghi, N., Buth, J.E., Au, C., Liu, Y., Lu, N., Du, P., Qin, F.X., Zhang, B., Gong, D., Dai, X., Sun, R., Novitch, B.G., Xu, Z., Qin, C.F., Cheng, G., 2017. 25-Hydroxycholesterol Protects Host against Zika Virus Infection and Its Associated Microcephaly in a Mouse Model. Immunity. 46 (3), 446–456.
Liu, S.Y., Aliyari, R., Chikere, K., Li, G., Marsden, M.D., Smith, J.K., Pernet, O., Guo, H., Nusbaum, R., Zack, J.A., Freiberg, A.N., Su, L., Lee, B., Cheng, G., 2013. Interferon-inducible cholesterol-25-hydroxylase broadly inhibits viral entry by production of 25-hydroxycholesterol. Immunity. 38 (1), 92–105.
Lund, E.G., Kerr, T.A., Sakai, J., Li, W.P., Russell, D.W., 1998. cDNA cloning of mouse and human cholesterol 25-hydroxylases, polytopic membrane proteins that synthesize a potent oxysterol regulator of lipid metabolism. J Biol Chem 273 (51), 34316–34327.
Moscona, A., 2005. Entry of parainfluenza virus into cells as a target for interrupting childhood respiratory disease. J Clin Invest. 115 (7), 1688–1698.
Murray, G.M., More, S.J., Sammin, D., Casey, M.J., McElroy, M.C., O'Neill, R.G., Byrne, W.J., Earley, B., Clegg, T.A., Ball, H., Bell, C.J., Cassidy, J.P., 2017. Pathogens, patterns of pneumonia, and epidemiologic risk factors associated with respiratory disease in recently weaned cattle in Ireland. J Vet Diagn Invest. 29 (1), 20–34.
Noton, S.L., Fearns, R., 2015. Initiation and regulation of paramyxovirus transcription and replication. Virology. 479–480 545-54.
Park, K., Scott, A.L., 2010. Cholesterol 25-hydroxylase production by dendritic cells and macrophages is regulated by type I interferons. J Leukocyte Biol. 88 (6), 1081–1087.
Qiu, X., Yu, Y., Yu, S., Zhan, Y., Wei, N., Song, C., Sun, Y., Tan, L., Ding, C., 2014. Development of strand-specific real-time RT-PCR to distinguish viral RNAs during Newcastle disease virus infection. Sci. World J. 2014, 934851.
Rasmussen, S.B., Reinert, L.S., Paludan, S.R., 2009. Innate recognition of intracellular pathogens: detection and activation of the first line of defense. APMIS. 117 (5-6), 323–337.
Schneider, W.M., Chevillotte, M.D., Rice, C.M., 2014. Interferon-stimulated genes: a complex web of host defenses. Annu. Rev Immunol. 32, 513–545.
Schoggins, J.W., Rice, C.M., 2011. Interferon-stimulated genes and their antiviral effector functions. Curr. Opin Virol. 1 (6), 519–525.
Schreiner, S., Wimmer, P., Dobner, T., 2012. Adenovirus degradation of cellular proteins. Future Microbiol. 7 (2), 211–225.
Shrivastava-Ranjan, P., Bergeron, E., Chakrabarti, A.K., Albarino, C.G., Flint, M., Nichol, S.T., Spiropoulou, C.F., 2016. 25-Hydroxycholesterol Inhibition of Lassa Virus Infection through Aberrant GP1 Glycosylation. mBio. 7 (6).
Song, Z., Zhang, Q., Liu, X., Bai, J., Zhao, Y., Wang, X., Jiang, P., 2017. Cholesterol 25-hydroxylase is an interferon-inducible factor that protects against porcine reproductive and respiratory syndrome virus infection. Vet. Microbiol. 210, 153–161.
Song, Z., Song, Z., Bai, J., Nauwynck, H., Lin, L., Liu, X., Yu, J., Jiang, P., 2019. 25-Hydroxycholesterol provides antiviral protection against highly pathogenic porcine reproductive and respiratory syndrome virus in swine. Vet. Microbiol. 231, 63–70.
Wang, X., Wang, P., Zhang, Z., Farre, J.C., Li, X., Wang, R., Xia, Z., Subramani, S., Ma, C.X., 2019. The autophagic degradation of cytosolic pools of peroxisomal proteins by a new selective pathway. Autophagy. 1–13.
Xiang, Y., Tang, J.J., Tao, W., Cao, X., Song, B.L., Zhong, J., 2015. Identification of Cholesterol 25-Hydroxylase as a Novel Host Restriction Factor and a Part of the Primary Innate Immune Responses against Hepatitis C Virus Infection. J. Virol. 89 (13), 6805–6816.
Yang, J., Zhao, G., Hou, P., Wang, H., LI, J., He, H., 2016. Esablishment and Preliminary Application of an Indirect ELISA for Detecting Antibodies against Bovine Parainfluenza Virus Type 3. Progress in Veterinary Medicine. 37 (11), 19–24 (in Chinese).
You, H., Yuan, H., Fu, W., Su, C., Wang, W., Cheng, T., Zheng, C., 2017. Herpes simplex virus type 1 abrogates the antiviral activity of Ch25h via its virion host shutoff protein. Antivir. Res. 143, 69–73.
Yvan-Charvet, L., Bonacina, F., Guinamard, R.R., Norata, G.D., 2019. Immunometabolic function of cholesterol in cardiovascular disease and beyond. Cardiovasc Res. 1755–3245.
Zhang, Y., Song, Z., Wang, M., Lan, M., Zhang, K., Jiang, P., Li, Y., Bai, J., Wang, X., 2019. Cholesterol 25-hydroxylase negatively regulates porcine intestinal coronavirus replication by the production of 25-hydroxycholesterol. Vet. Microbiol. 231, 129–138.
Zhao, G., Hou, P., Huan, Y., He, C., Wang, H., He, H., 2018a. Development of a recombinase polymerase amplification combined with a lateral flow dipstick assay for rapid detection of the Mycoplasma bovis. BMC Vet. Res. 14 (1), 412.
Zhao, G., Wang, H., Hou, P., He, C., He, H., 2018b. Rapid visual detection of Mycobacterium avium subsp. paratuberculosis by recombinase polymerase amplification combined with a lateral flow dipstick. J. Vet Sci. 19 (2), 242–250.
Zhao, G., He, H., Wang, H., 2019. Use of a recombinase polymerase amplification commercial kit for rapid visual detection of Pasteurella multocida. BMC Vet. Res. 15 (1), 154.